Noise Filtering for Highly Correlated Photon Pairs From Silicon Waveguides

Jong-Moo Lee, Wook-Jae Lee, Min-Su Kim, and Jung Jin Ju

***Abstract*—We fabricate silicon waveguide spirals and a ring resonator to generate photon pairs based on a spontaneous four-wave mixing. The coincidence-to-accidental-ratio (CAR) of photon pairs from the silicon waveguides is measured up to 400 after a noise-filtering by using the combination of bandpass filters and pump-rejection filters. The CAR is enhanced up to 700 by adding on-chip pump-rejection MZIs. We observe the CAR of the photon pairs from a silicon spiral is highly depending on the wavelength detuning from the pump wavelength. We discuss the noise sources related to the degradation of the CAR based on our experimental results.**

***Index Terms*—Integrated optics, optical planar waveguides, quantum optics.**

I. Introduction

SILICON photonics technology is an attractive candidate to realize a quantum information processing platform including a quantum-correlated photon-pair source [1]–[8], wavelength filters [9]–[13], and quantum interference circuits [14]–[16]. Generation of quantum-correlated photon pairs has been reported based on a spontaneous four-wave mixing (SFWM) with a strong pump field through a silicon photonic waveguide [1]–[8]. The photon pairs are relatively weak compared to the co-propagating pump field and should be filtered by high-extinction pump-rejection filters (PRFs) to be useful for the quantum information processing.

Several fiber-coupled dielectric filters connected in series can be used as the high-extinction PRF [1]–[8] but the integration of PRFs on a single chip [9]–[13] together with the silicon waveguide photon pair source is highly attractive toward a fully integrated quantum processing platform. Arrayed waveguide gratings [9], ring resonators [10], [11], Bragg filters [14], and cascaded Mach-Zehnder interferometers (MZIs) [12], [13] have been tried to realize the on-chip integration of PRFs.

The correlation quality of a photon-pair source can be estimated by coincidence-to-accidental-ratio (CAR) which is the ratio of correlated events of the photon pairs to the system noise [4]–[11]. The CAR of photon pairs from silicon waveguides has been reported to be depending on the pumping power in addition to the quality of the pump and noise rejection [7], [8].

Manuscript received May 9, 2019; revised August 14, 2019; accepted September 16, 2019. Date of publication September 19, 2019; date of current version November 1, 2019. This work was supported by Institute for Information & Communications Technology Promotion under Grant 20170000740011001 funded by MSIT. *(Corresponding author: Jong-Moo Lee.)*

The authors are with the Electronics and Telecommunications Research Institute, Daejeon 34129, South Korea (e-mail: jongmool@etri.re.kr; lee.wookjae@etri.re.kr; kimms@etri.re.kr; jjju@etri.re.kr).

Color versions of one or more of the figures in this article are available online at http://ieeexplore.ieee.org.

Digital Object Identifier 10.1109/JLT.2019.2942436

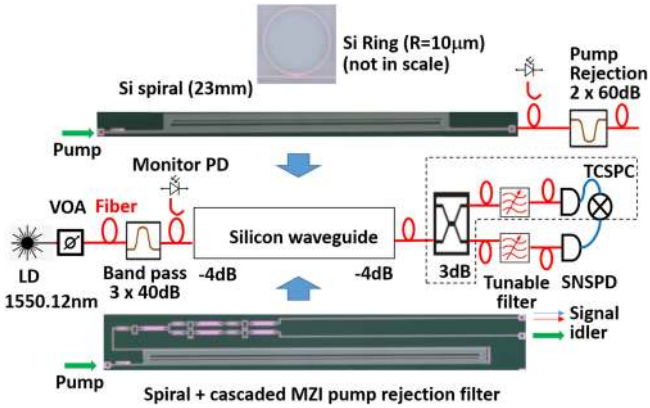

Fig. 1. Experimental schematic to measure CAR of photon pairs and microscopic images of two silicon waveguide spirals and a ring resonator. One spiral is followed by on-chip cascaded MZIs as a pump-rejection filter (PRF), and the other is connected to external fiber-coupled PRFs.

In this paper, we generate photon pairs from silicon waveguides based on SFWM and measure the CAR of the photon pairs up to 400 after a noise-filtering by the combination of bandpass filters and pump-rejection filters. We also integrate on-chip cascaded MZIs following a silicon waveguide spiral on a single chip, and demonstrate the enhancement in CAR of the photon pairs up to 700 by adding the on-chip pump-rejection MZIs. We measure the variation of the CAR depending on the wavelength detuning from the pump and discuss the noise sources degrading the CAR including spontaneous Raman scattering (SpRS) [18]–[21] and other noise spectrum sources.

II. Experimental Setup

Our design of integrated photonic circuits was fabricated at IMEC/Europractice using their passive Silicon-on-Insulator (SOI) platform. The cross-sectional dimension of the SOI waveguide is 550 × 220 nm in our design and vertical grating couplers (VGCs) are used to couple the light between optical fibers and the waveguide at the average loss of 4 dB/facet at 1550 nm wavelength.

Figure 1 shows the experimental setup and microscopic images of two silicon waveguide spirals and a ring resonator to generate photon pairs based on the SFWM. One of the two spiral waveguides in Fig. 1 is followed by on-chip cascaded MZIs as a PRF and the other is connected to a series of external

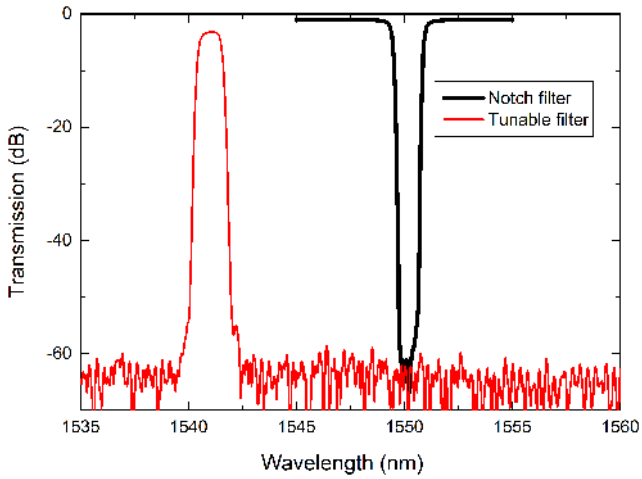

Fig. 2. Measured transmission spectra through one of the double notch filters for the external PRFs and the tunable bandpass filter selecting the wavelength band passing to the SNSPD, respectively.

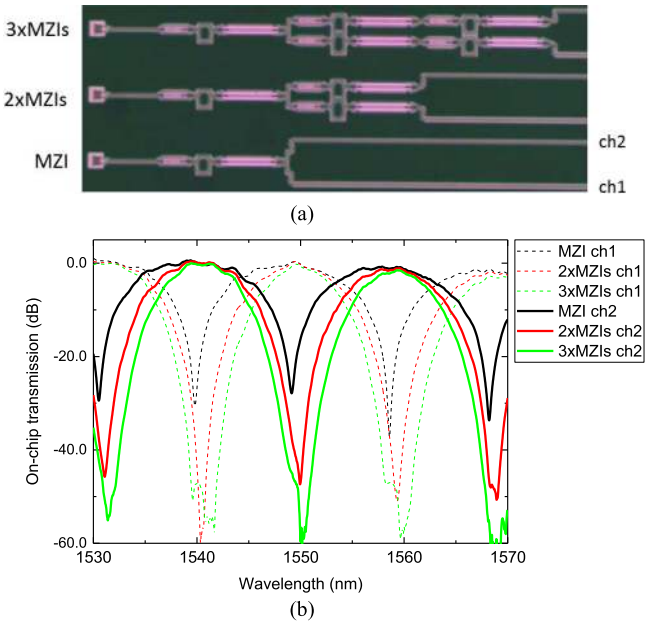

Fig. 3. Microscopic image showing a single MZI, double-cascaded MZIs (2xMZIs), and triple-cascaded MZIs (3xMZIs) to reject the pump wavelength in (a), and the measured transmission spectra of the MZIs in (b).

fiber-coupled PRFs. We used a fiber-coupled continuous-wave (CW) laser diode (LD) (Thorlabs, SFL1550P) emitting a single wavelength mode at 1550.12 nm as the pumping source for the SFWM. We fixed the optical power from the LD as 40 mW and used a variable optical attenuator to control the optical power to the SOI waveguide. Three fiber-coupled 200 GHz optical bandpass filters (BPFs) with channel isolation over 40 dB per each and the insertion loss of 1 dB per each were connected in series and used to suppress the background photons from the LD.

The length of the waveguide spirals is 23 mm. Triple-cascaded or quadruple-cascaded MZIs were integrated following the spiral to separate out the co-propagating pump after the photon-pair generation by the SFWM. The external PRFs connected to the spiral without on-chip filters were composed of two fiber-coupled 200 GHz optical notch filters with the channel isolation over 60 dB per each and the insertion loss of 1 dB per each.

A fiber-coupled 3-dB coupler was used to non-deterministically split the photon pairs into separate superconducting nanowire single-photon detectors (SNSPDs) [22]. Two tunable bandpass filters (EXFO, XTM-50) with the 3-dB bandwidth of 1 nm were used to select the wavelength of the signal and idler pair and a time-correlated single-photon counter (TCSPC) was used to estimate the CAR of the photon pairs.

Figure 2 shows the measured transmission spectra through one of the double notch filters for the external PRFs and the tunable bandpass filter selecting the wavelength band passing to the SNSPD, respectively.

III. Transmission Spectrum of MZI Filters

Figure 3 shows the microscopic image of a single MZI, double-cascaded MZIs (2xMZIs), and triple-cascaded MZIs (3xMZIs), and the measured transmission spectra through the MZIs. The single MZI includes 1×2 and 2×2 multi-mode interference (MMI) structure. The cascaded MZIs in Fig. 3 are composed of the identical MZIs to separate out the pump wavelength to a channel (ch1 in Fig. 3) as much as possible and keep the photon pairs to the other channel (ch2 in Fig. 3) with a minimal insertion loss.

We measured the transmission spectra by using a broadband source and the on-chip transmission was estimated in comparison with the transmission through a straight waveguide and the VGCs for coupling to the fibers. Measured results in Fig. 3 show that the extinction ratio increases by the repetition of the MZIs in series. The on-chip transmission loss through the 3xMZIs was measured less than 1 dB at the wavelength 1541 and 1559 nm, and the extinction ratio was measured close to 60 dB at 1550.12 nm which is in accord with the wavelength of the pump LD to generate photon pairs.

Figure 4 shows the microscopic image of a spiral followed by a 3xMZIs and a spiral followed by quadruple-cascaded MZIs (4xMZIs), and the measured transmission spectra through them. The measured on-chip transmission in Fig. 4 includes the propagation loss of the 23 mm waveguide spiral in addition to the insertion loss of the cascaded MZIs.

The extinction ratio was measured at about 55 dB at 1550.12 nm. The measured extinction ratio is close to the sensitivity limit of the optical spectrum analyzer (OSA) (ANDO AQ6317) used in this measurement. The insertion loss of the spiral was estimated as 4.6 dB considering the waveguide propagation loss of 0.2 dB/mm. The insertion loss is about 6 dB through the spiral and 3xMZIs, about 10 dB through the spiral and 4xMZIs at the wavelength 1541 and 1559 nm. The extra loss of the 4xMZIs is due to the design of the last MZI of the 4xMZIs are not identical to the other three MZIs in front. The last MZI of the 4xMZIs was designed with the free-spectral range (FSR) twice wider than the others.

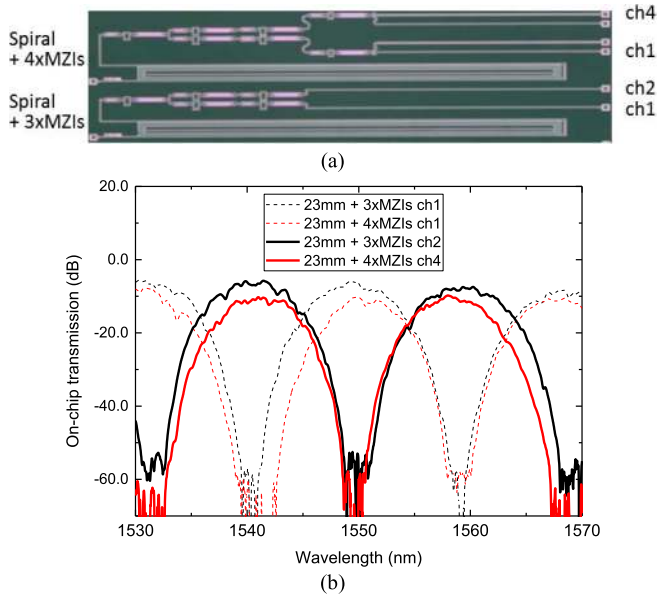

Fig. 4. Microscopic image of a spiral followed by triple-cascaded MZIs (3xMZIs) and a spiral followed by quadruple-cascaded MZIs (4xMZIs) in (a), and the measured transmission spectra through the combinations of the spiral and MZIs in (b).

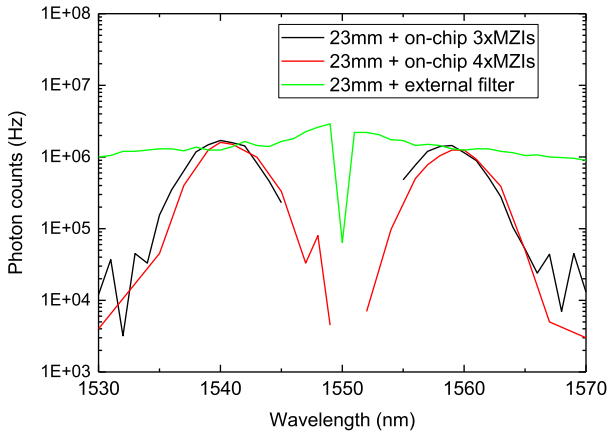

Fig. 5. Measured photon counts of the silicon waveguide spiral followed by on-chip 3xMZIs and 4xMZIs, in comparison with a spiral followed by external fiber-coupled PRFs instead of the on-chip MZIs.

IV. Photon-Pair Generation

A. Photon-Pair Generation From a Silicon Spiral

Figure 5 shows the spectrum of photon counts measured by using an SNSPD, for a spiral and external PRF, the spiral and 3xMZIs, and the spiral and 4x MZIs, respectively. We used the experimental setup in Fig. 1, but without the 3-dB coupler in front of the tunable filter for the measurement in Fig. 5. We measured the photon counts at 1-nm steps from 1530 nm to 1570 nm by scanning the bandpass wavelength of the tunable filter.

Measured results in Fig. 5 show that photon pairs are counted over 1 MHz/nm at 8.6 mW of pump power coupled to the silicon waveguide. The residual pump was suppressed very well by the external PRFs by showing a dip at the pump wavelength for the combination of the spiral and external PRFs in Fig. 5. The cascaded MZIs suppressed the residual pump enough for the measurement and separate the photon pairs without a critical loss at the wavelength of the signal and idler wavelengths, 1541 and 1559 nm, respectively. The 4xMZIs was much better in suppressing the residual pump than the 3xMZIs and we could measure the photon counts as close as 1 nm in wavelength to the pump for the 4xMZIs.

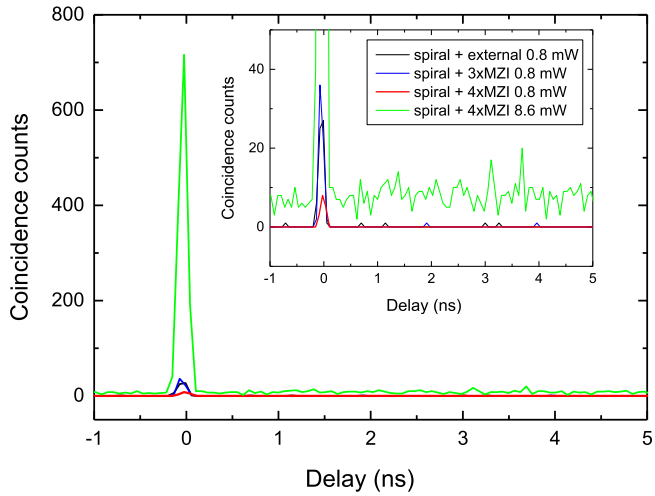

Fig. 6. Measured coincidence counts of the photon pairs from the silicon waveguide spiral followed by the on-chip 3xMZIs and 4xMZIs, respectively, in comparison with the spiral followed by the external fiber-coupled PRFs instead of the on-chip MZIs. The wavelength of 1541.1 nm for the signal and 1559.1 nm for the idler with the bandwidth of 1 nm were filtered by the tunable filters in the measurement.

Figure 6 shows the measured coincidence counts of the photon pairs from the silicon waveguide spiral followed by the on-chip 3xMZIs and 4xMZIs, respectively, in comparison with the spiral followed by the external fiber-coupled PRFs instead of the on-chip MZIs. We used two SNSPDs to detect the photon pairs non-deterministically split by the 3-dB coupler and a TCSPC to measure the coincidence counts as in the experimental setup in Fig. 1. The wavelength of 1541.1 nm for the signal and 1559.1 nm for the idler with the bandwidth of 1 nm were filtered by the tunable filters in the measurement. We used the tunable filters with 60 dB extinction in both experiments with the external PRFs and with the MZI PRFs instead of the external PRFS, respectively. The tunable filter added 60 dB extinction to the pump rejection of 55 dB through the on-chip MZI PRFs.

The coincidence counts in Fig. 6 shows the coincidence events per time-bin of 64 ps for the measurement duration of 1 sec. The coincidence counts decrease down to several tens from 700 but the accidental counts also decrease, as the pump power reduced down to 0.8 mW from 8.6 mW. No accidental coincidence counts are visible for the spiral and 4xMZIs at 0.8 mW pump power in Fig. 6.

The correlation quality of the photon pairs can be estimated by calculating the CAR from the measured coincidence counts. We calculated the CAR from the coincidence counts by comparing with average accidental coincidence counts for the delay up to

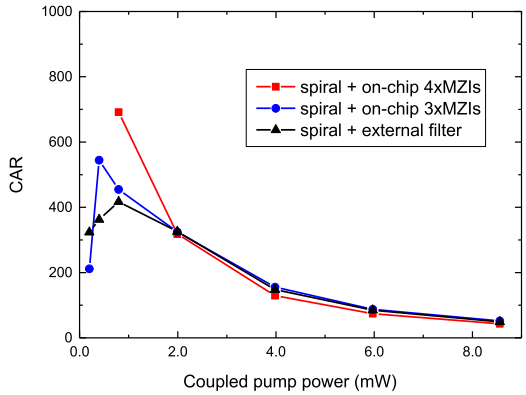

Fig. 7. Measured coincidence-to-accidental ratio (CAR) of the photon pairs from a silicon waveguide spiral followed by the on-chip 3xMZIs and 4xMZIs, in comparison with a spiral followed by the external fiber-coupled PRFs instead of the on-chip MZIs.

100 ns. Figure 7 shows the CAR of photon pairs depending on the pump power coupled to the waveguides, for the silicon waveguide spiral followed by the on-chip 3xMZIs and 4xMZIs, respectively, in comparison with the spiral followed by the external fiber-coupled PRFs instead of the on-chip MZIs.

The calculated CAR in Fig. 7 increases from 50 at 8.6 mW pump to 400 for the spiral with the external filters, 450 for the spiral with the on-chip 3xMZIs, and 700 for the spiral with the on-chip 4xMZIs at 0.8 mW pump power. Fig. 7 clearly shows that CAR is enhanced at low pump powers by using the on-chip PRFs instead of the external PRFs.

B. Photon-Pair Generation From a Ring Resonator

The silicon chip in this experiment is including a ring resonator with a radius of 10 μm and a gap of 200 nm. We measure photon-pair generation from the ring resonator for comparison, by replacing the spiral in Fig. 1 with the ring resonator.

Figure 8 shows the measured spectrum of the photon counts from the silicon ring resonator at the pump power of 0.6 mW and 8.1 mW, in comparison with its resonance transmission spectrum. Figure 8 clearly shows that the photon pairs are generated at the resonance wavelength of the ring resonator. The photon-pair generation at the resonance wavelengths is saturated as the pump power increases and the photon pair generation from the straight waveguide grows at the wavelengths between the resonant wavelengths.

Figure 9 shows the measured CAR at the resonant wavelength together with the coincidence and accidental counts of the photon pairs from the silicon ring resonator. Figure 9 shows that the coincidence counts rapidly increase at a low pump power but are saturated as the pump power increased. CAR of the ring resonator is measured as high as the CAR of the silicon spiral at a low pumping power.

V. Discussion on Noise Sources

A. Noise by Spontaneous Raman Scattering

We need to study noise sources to understand the difference in CAR for the spiral with and without the on-chip PRFs. The main

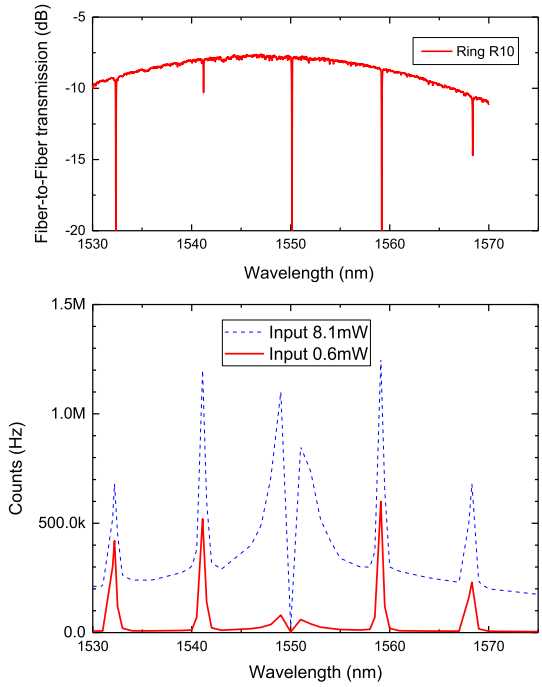

Fig. 8. Measured spectrum of the photon counts from the silicon ring resonator at the pump power of 0.6 mW and 8.1 mW, in comparison with its resonance transmission spectrum.

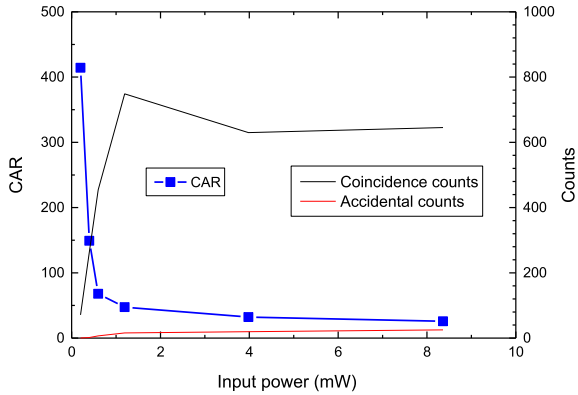

Fig. 9. Measured CAR of the photon pairs from the silicon ring resonator together with the coincidence and accidental counts.

difference in the experimental setup is the optical fiber between the spiral generating photon pairs and the PRFs.

We measure the photon-counting spectrum of pump light through the bandpass filter followed by the fiber and the external PRFs (BPF-Fiber-PRF), in comparison with the spectrum through the external PRFs followed by the fiber and the bandpass filter in reverse order (PRF-Fiber-BPF) as in Fig. 10. The length of the fiber was 4 m in the experiment.

The measured spectrum for the PRF-Fiber-BPF in Fig. 10 shows only the wavelength peak of the residual pump suppressed enough by the PRFs. The measured spectrum for the BPF-Fiber-PRF in Fig. 10 shows a broad spectrum of Stokes and anti-Stokes signal with peaks at about ± 1 THz shifted from the pump wavelength, and it is well in accord with the SpRS

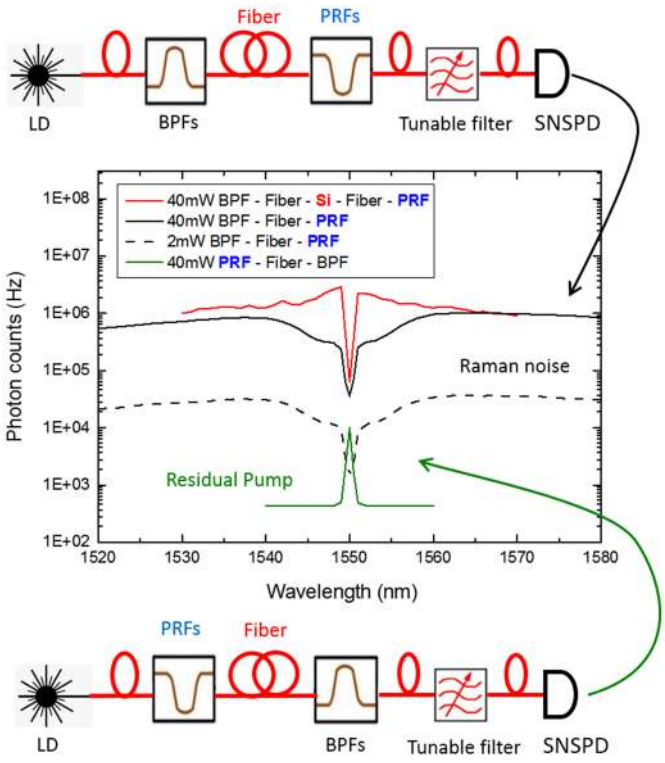

Fig. 10. Measured photon counts of 40 mW pump light through the bandpass filter followed by a fiber and the external PRFs (40 mW BPF-Fiber-PRF), in comparison with the spectrum through the external PRFs followed by the fiber and the bandpass filter in reverse order (40 mW PRF-Fiber-BPF). Measured photon counts for the silicon waveguide spiral followed by the external fiber-coupled PRFs at the same pump power are also shown for a comparison (40 mW BPF-Fiber-Si-Fiber-PRF). Measured photon counts of 2 mW pump light through the bandpass filter followed by the fiber and the external PRFs (2 mW BPF-Fiber-PRF) are also shown for a comparison.

spectrum through an optical fiber as reported in ref [18]–[20]. The measured SpRS spectrum shows that an extra noise can be generated by the optical fiber between the silicon chip and the external PRFs.

We showed photon-counting spectrum for the silicon waveguide spiral followed by the external fiber-coupled PRFs to compare the photon counts by SFWM through the silicon waveguide with the photon counts by SpRS through the optical fiber. The extra loss of 12.5 dB by the insertion of the silicon chip should be considered in estimating the SpRS noise. We measured the photon counts of 2 mW pump light through the bandpass filter followed by the fiber and the external PRFs (2 mW BPF-Fiber-PRF), to estimate the SpRS noise level with the insertion of the silicon chip as in Fig. 10.

Figure 11 shows the measured photon counts depending on the pump power and the quadratic fit of the measured data for the silicon waveguide spiral followed by the external fiber-coupled PRFs, in comparison with the Raman noise through the fiber which increases linearly depending on the pump power.

The influence of the Raman noise is more critical for the low pump power because SpRS is linearly increase depending on the pump power, while the photon-pair generation shows a quadratic growth depending on the pump power. This explains

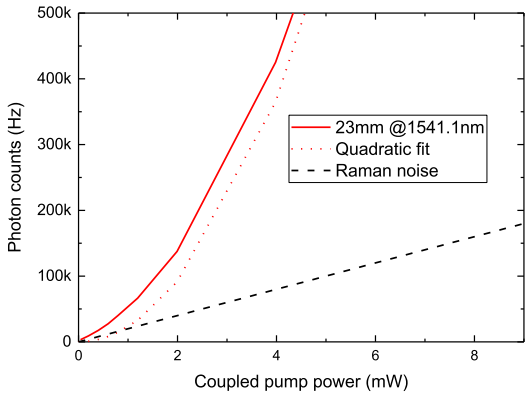

Fig. 11. Measured photon counts and the quadratic fit for the silicon waveguide spiral followed by the external fiber-coupled PRFs, in comparison with the Raman noise through the fiber which increases linearly depending on the pump power.

why the difference in CAR is clearly observed in low pumping powers in our experimental results as in Fig. 7. The results show that the on-chip integration of PRFs is beneficial to improve the correlation of the photon pairs by removing extra noise of SpRS induced by the residual pump through the optical fiber connected to the silicon chip.

B. *Noise Spectrum Close to the Pump Wavelength*

The measured spectrum of photon counts from silicon waveguides in Fig. 8 and Fig. 10 shows relatively high photon counts for the wavelength slightly detuned by 1∼2 nm from the pump wavelength. The origin of the high photon counts near the pump wavelength is not clearly understood. The bandwidth of SFWM is known to be as broad as several 10 s of nm. The detuning of 1∼2 nm is too close to the pump for Raman scattering and too far for Brillouin scattering. The origin of the high photon counts is not clearly understood but we observe that those photons are critical noise sources degrading the CAR of correlated photon pairs.

Figure 12 shows the measured spectrum of photon counts from silicon waveguide with the various lengths of 0.5, 2, 12, and 23 mm, in comparison with the measured CAR for the 23-mm long waveguide depending on the wavelength detuning of 1, 2, and 9 nm from the pump wavelength. The measured CAR in Fig. 12 shows critical degradation for the wavelength close to the photon-counting peak near the pump wavelength.

The increase of the photon-counting peak for the long length of the waveguide in Fig. 12 shows that the origin of the photon-counting peak is not the residual pump power but an inelastic scattering through the silicon waveguide. The origin of the photon-counting peak is not clearly understood but the measured result shows that the photon-counting peak is including a big portion of a noise source in addition to correlated photon pairs. So, we need to avoid the several-nm width of the wavelength band near the photon-counting peak to get highly correlated photon pairs from the silicon waveguides.

Clemmen *et al.* also observed and analyzed the SpRS noise from an optical fiber and the noise spectrum at small detuning

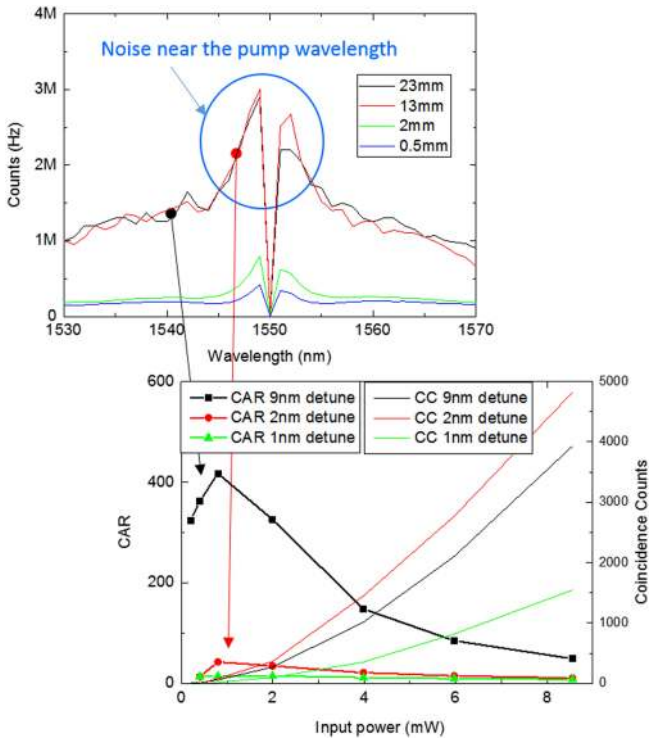

Fig. 12. Measured spectrum of photon counts from silicon waveguide with the various lengths of 0.5, 2, 12, and 23 mm, in comparison with the measured CAR for the 23-mm long waveguide depending on the wavelength detuning of 1, 2, and 9 nm from the pump wavelength.

from the pump wavelength, as in [21]. Our analysis of SpRS noise through an optical fiber is very well in accord with their results. The noise spectrum at small detuning from the pump wavelength is regarded due to inelastic scattering of the pump beam on a one-dimensional thermal bath of excitations, even though the origin of the scattering is unclear [21]. They also reported that the noise was not related to the free-carrier density because the temporal response of the noise flux was faster than the free-carrier dynamics [21]. The results in [21] and our results are well in accord in showing the influence of the unknown noise source from SOI waveguide at small detuning and the SpRS noise from the optical fiber at large detuning from the pump wavelength. The influence of both noise sources at the small and large detuning is expected to be similar in pulse pumping considering the temporal response of both noise sources faster than the free-carrier dynamics.

In this experiment, we reduced the SpRS noise from the optical fiber by using the on-chip pump-rejection filters integrated with the SOI spiral waveguide. We selected the bandwidth away from the inelastic pump noise at small detuning from the pump wavelength by using the external tunable filter. The combined effect of the on-chip pump-rejection and the bandwidth selection by the external tunable filter contributed to the correlation quality of the photon pair improved in CAR up to 700.

VI. Conclusion

We fabricated silicon waveguide spirals and a ring resonator to generate photon pairs based on the spontaneous four-wave mixing. The CAR of photon pairs from the silicon waveguides was measured at about 400 after a noise-filtering by using the combination of bandpass filters and pump-rejection filters. The CAR was enhanced up to 700 by adding on-chip pump-rejection MZIs. We observed that CAR of the photon pairs highly depends on the wavelength detuning from the pump wavelength. One of the noise sources degrading the CAR is the spontaneous Raman scattering through the optical fiber coupled to the silicon waveguide, and there is an additional noise source close to the pump wavelength. In conclusion, we need to avoid the several-nm width of noise spectrum near the pump wavelength in addition to rejecting the residual pump power and the spontaneous Raman scattering, to get highly correlated photon pairs.

References

[1] J. W. Silverstone, D. Bonneau, J. L. O'Brien, and M. G. Thompson, "Silicon quantum photonics," *IEEE J. Sel. Topics Quantum Electron.*, vol. 22, no. 6, Nov./Dec. 2016, Art. no. 6700113.

[2] Q. Lin and G. P. Agrawal, "Silicon waveguides for creating quantum-correlated photon pairs," *Opt. Lett.*, vol. 31, pp. 3140–3141, 2006.

[3] J. E. Sharping *et al.*, "Generation of correlated photons in nanoscale silicon waveguides," *Opt. Express*, vol. 14, pp. 12388–12393, 2006.

[4] H. Takesue *et al.*, "Entanglement generation using silicon wire waveguide," *Appl. Phys. Lett.*, vol. 91, 2007, Art. no. 201108.

[5] K. Harada *et al.*, "Generation of high-purity entangled photon pairs using silicon wire waveguide," *Opt. Express*, vol. 16, pp. 20368–20373, 2008.

[6] S. Clemmen, K. P. Huy, W. Bogaerts, R. G. Baets, Ph. Emplit, and S. Massar, "Continuous wave photon pair generation in silicon-on-insulator waveguides and ring resonators," *Opt. Express*, vol. 17, pp. 16550–16570, 2009.

[7] K. Guo *et al.*, "High coincidence-to-accidental ratio continuous-wave photon-pair generation in a grating-coupled silicon strip waveguide," *Appl. Phys. Express*, vol. 10, 2017, Art. no. 062801.

[8] C. Ma, X. Wang, V. Anant, A. D. Beyer, M. D. Shaw, and S. Mookherjea, "Silicon photonic entangled photon-pair and heralded single photon generation with CAR $>$ 12,000 and $g^{(2)}(0) < 0.006$," *Opt. Express*, vol. 25, pp. 32995–33006, 2017.

[9] N. Matsuda *et al.*, "On-chip generation and demultiplexing of quantum correlated photons using a silicon-silica monolithic photonic integration platform," *Opt. Express*, vol. 22, pp. 22831–22840, 2014.

[10] N. C. Harris *et al.*, "Integrated source of spectrally filtered correlated photons for large-scale quantum photonic systems," *Phys. Rev. X*, vol. 4, 2014, Art. no. 041047.

[11] C. M. Gentry *et al.*, "Monolithic source of entangled photons with integrated pump rejection," in *Proc. Conf. Lasers Electro-Opt.*, 2018, Paper Jth4C.3.

[12] C. M. Wilkes *et al.*, "60 dB high-extinction auto-configured Mach–Zehnder interferometer," *Opt. Lett.*, vol. 41, pp. 5318–5321, 2016.

[13] M. Piekarek *et al.*, "High-extinction ratio integrated photonic filters for silicon quantum photonics," *Opt. Lett.*, vol. 42, pp. 815–818, 2017.

[14] D. Perez-Galacho *et al.*, "Optical pump-rejection filter based on silicon sub-wavelength engineered photonic structures," *Opt. Lett.*, vol. 42, pp. 1468–1471, 2017.

[15] J. Carolan *et al.*, "Universal linear optics," *Science*, vol. 349, pp. 711–716, 2015.

[16] I. I. Faruque, G. F. Sinclair, D. Bonneau, J. G. Rarity, and M. G. Thompson, "On-chip quantum interference with heralded photons from two independent micro-ring resonator sources in silicon photonics," *Opt. Express*, vol. 26, pp. 20379–20395, 2018.

[17] X. Qiang *et al.*, "Large-scale silicon quantum photonics implementing arbitrary two-qubit processing," *Nature Photon.*, vol. 12, pp. 534–539, 2018.

[18] Q. Lin, F. Yaman, and G. P. Agrawal, "Photon-pair generation in optical fibers through four-wave mixing: Role of Raman scattering and pump polarization," *Phys. Rev. A*, vol. 75, 2007, Art. no. 023803.

[19] N. A. Peters *et al.*, "Dense wavelength multiplexing of 1550 nm QKD with strong classical channels in reconfigurable networking environments," *New J. Phys.*, vol. 11, 2009, Art. no. 045012.

[20] A. S. Clark, M. J. Collins, A. C. Judge, E. C. Magi, C. Xiong, and B. J. Eggleton, "Raman scattering effects on correlated photon-pair generation in chalcogenide," *Opt. Express*, vol. 20, pp. 16807–16814, 2012).
[21] S. Clemmen *et al.*, "Low-power inelastic light scattering at small detunings in silicon wire waveguides at telecom wavelengths," *J. Opt. Soc. Amer. B*, vol. 29, pp. 1977–1982, 2012.
[22] E. A. Dauler *et al.*, "Review of superconducting nanowire single-photon detector system design options and demonstrated performance," *Opt. Eng.*, vol. 53, 2014, Art. no. 081907.

Jong-Moo Lee received the BS degree from Seoul National University, Seoul, South Korea, in 1991, and the M.S. and Ph.D. degrees in a femtosecond fiber laser from Korea Advanced Institute of Science and Technology, Daejeon, South Korea, in 1993 and 1997, respectively. He joined Electronics and Telecommunications Research Institute (ETRI) in 2001 after his industrial experiences at LG IS Co., Ltd. and EO Technics Co., Ltd. In ETRI, his research activity has been on planar waveguide devices for optical communication, such as arrayed waveguide gratings, wavelength filters, and optical transceivers. His current research topic is silicon photonic devices.

Wook-Jae Lee, biography not available at the time of publication.

Min-Su Kim received the B.S., M.S., and Ph.D. degrees in physics from Korea Advanced Institute of Science and Technology (KAIST), Daejeon, South, in 1993, 1995, and 2002, respectively. In KAIST, he carried out theoretical and experimental researches related to various second- and third-order nonlinear optical processes. He joined Electronics and Telecommunications Research Institute, in 2002, where he has been engaged mainly in the research on functional optical devices related with nonlinear optical processes and planar waveguide structures. He is recently involved with thermal analyses of dielectric and silicon photonic waveguide devices.

Jung Jin Ju received the B.S., M.S., and Ph.D. degrees from the Physics Department, Pusan National University, Busan, South Korea, in 1990, 1992, and 1997, respectively. He studied laser spectroscopy of rare-earth ions doped solids and second-order nonlinear optics of dielectric crystals. From 1997 to 2000, he was a Postdoctoral Researcher with the Korea Research Institute of Standards and Science, responsible for the development of optical high-temperature sensors for engine diagnostics, and also with Pohang University of Science and Technology, Pohang, South Korea, where he conducted research about THz source development. Since August 2000, he has been a Senior Researcher with the Electronics and Telecommunications Research Institute, Daejeon, South Korea. His research interests include polymeric waveguide devices for optical communications, plasmonic devices for optical interconnects, and quantum optics based on integrated photonics.